

Electronic Supplementary Information
for
X-ray diffraction for probing free energy profiles
and self-diffusivity of gases in metal-organic
frameworks

Da-Shiuan Chiou^a, Yu-Chun Chuang^b, Chung-Kai Chang^b, Cheng-Hsun Hsu^a, Li-Chiang Lin^a
and Dun-Yen Kang^{a,*}

^a*Department of Chemical Engineering, National Taiwan University, No. 1, Sec. 4, Roosevelt Road, Taipei
10617, Taiwan*

^b*National Synchrotron Radiation Research Center, 101 Hsin-Ann Road, Hsinchu, 30076 Taiwan*

E-mail: dunyen@ntu.edu.tw

Methods

Chemicals and materials

Isophthalic acid (1,3-H₂BTC, 99%) was purchased from Alfa Aesar. Aluminum sulfate 18-hydrate (Al₂(SO₄)₃·18H₂O) was purchased from JT Baker. *N,N*-dimethylformamide (DMF, 99.8%) and methanol (MeOH, 99%) were purchased from Macron. All reagents and solvents were used as received without further purification. Deionized water (DI water) was obtained using the ELGA VEOLIA PURELAB analytical ultrapure water system.

Synthesis of CAU-10-H powder

Al₂(SO₄)₃·18H₂O (3.332 g, 5 mmol) and 1,3-H₂BTC (0.8306 g, 5 mmol) were dissolved in a mixed solvent of DI water (24 mL) and DMF (6 mL). The solution was stirred and refluxed at 120 °C for 2 days. White powder that formed during the reaction was collected via vacuum filtration and rinsed using DI water. Activation of as-synthesized CAU-10-H (i.e., removal of DMF from micropores) was achieved by immersing powder samples in methanol (50 mL) at room temperature under agitation for 1 day. The samples were collected via vacuum filtration and dried at 105 °C for 1 day prior to use.

X-ray diffraction with synchrotron radiation source

Time-resolved *in situ* X-ray diffraction (XRD) measurements of CAU-10-H exposed to CO₂ and CH₄ were conducted at Taiwan Photon Source (TPS) stations 09A and 19A at the National Synchrotron Radiation Research Center (NSRRC). The wavelengths of the incident X-rays were

0.826569 Å (15 keV) and 0.77489 Å (16 keV) at Stations 09A and 19A, respectively. The X-ray were delivered from in-vacuum undulators: IU22 (Station 09A) and CU15 (Station 19A). The diffraction patterns were recorded using position-sensitive detectors: MYTHEN 24K (Station 09A) and MYTHEN 18K (Station 19A). Powder samples were packed in a capillary tube with a diameter of 0.7 mm. Measurements were performed using a proprietary setup (Fig. S7). CO₂ or CH₄ was introduced into the capillary tube after degassing the entire system at 0.005 bar for 6 h. The XRD patterns were obtained under an atmosphere of CO₂ at 0.5, 1, or 3 bar at 303 K as well as under 3 bar at 343 K. For measurements involving CH₄, the diffraction patterns were acquired at 0.5, 1, and 3 bar of CH₄ at 303 K. All of the XRD patterns were recorded following an exposure duration of 1 s.

Electron density map derived using XRD-based method

Rietveld refinement was performed using the GSAS II program with each powder XRD pattern sample under different atmospheric conditions.¹ The crystallographic information file (CIF) obtained from Cambridge Crystallographic Data Centre (CCDC) under a deposition number of 1454067 was adopted as the initial structure in this analysis.² The background was modeled as a 10th-order polynomial equation. The analysis of Rietveld refinement on the XRD pattern ranging from 3-20° 2 θ yielded a structure factor in the reciprocal space, F_o , describing the crystal structure of the MOF. The maximum entropy method (MEM) was applied to the same XRD patterns using the software application Dysnomia combined in GSAS II program.³ The grid size was set to be 0.5 Å, and the peak cutoff was set to be 10%. This yielded another structure factor in the reciprocal space: F_c . Unlike F_o , this factor contains spatial information related to both the MOF and the

adsorbed gas molecules (CO_2 or CH_4). Subtracting F_c from F_o yielded F_{delt} , which retained only the spatial information related to adsorbed gas molecules in the reciprocal space. The inverse Fourier transform was applied to F_{delt} using the software application, VESTA,⁴ in order to obtain the electron density of the gas molecules in the real space. The aforementioned method for deriving the electron density maps is referred to as XRD-based in the main text, and is illustrated in Fig. S1 along with the MC-based method. The electron density maps were then converted to the probability distributions of a gas species in the MOF, which could be further used to derive the Helmholtz free energy profiles. In this study, the 2D probability distributions for a gas molecule had a spatial resolution of 1 pixel per $0.5 \text{ \AA} \times 0.5 \text{ \AA}$, while the 1D ones had a resolution of 1 data point per 0.5 \AA . The relationship between the probability distribution and the Helmholtz free energy is described in the main text (eq. 1-3)

Monte Carlo simulations

The adsorption of CO_2 and CH_4 on CAU-10-H was also computed using the Monte Carlo (MC) simulations in the grand canonical ensemble at various pressures (0.5, 1, and 3 bar) at 303K and 343K. The MC simulations yielded information pertaining to the distribution of gas molecules in the MOF structure. In MC computation, we applied 6–12 Lennard-Jones (L–J) potential after truncation and shifting at a cutoff radius of 12 \AA . Long-range Coulombic interactions were computed using the Ewald summation method to describe intermolecular interactions. The simulation box comprised multiple unit cells to ensure that the side length in each direction was at least twice the cutoff radius. The derivation of L–J parameters of atoms in the MOF was based on the DREIDING force field (Table S3).⁵ The Lorentz–Berthelot mixing rule was used for the

assignment of L–J parameters between dissimilar atoms. For each MC simulation, at least 100,000 cycles were performed. The electron density maps were obtained from the results with 3,000 cycles of MC calculation.

Calculations of density functional theory

The electron density distribution of CO₂ and CH₄ was computed in accordance with density functional theory (DFT). The resulting electron density distributions enabled the conversion of molecular contours obtained from MC simulations into electron density maps, as detailed in the preceding section. The aforementioned method is referred to as the MC-based method in the main text. The DFT calculations were performed using the CASTEP module in the Material Studio software.^{6, 7} Generalized gradient approximation applying Perdew–Burke–Ernzerhof functional was used to describe exchange and correlation interactions.⁸ Ultra-soft pseudopotential was used to describe the interactions between electrons and ionic cores.⁹ BFGS optimization algorithm was used for geometry optimization with one gas molecule placed in a 12 × 12 × 12 Å³ box under periodic boundary conditions.¹⁰ The electronic wave function was expanded on a plane wave basis with cut-off energies of 340 eV for CO₂ and 280 eV for CH₄. The convergence criteria for geometry optimization included the following: a) self-consistent field of 1.0×10⁻⁶ eV/atom, b) energy of 1 × 10⁻⁵ eV/atom, c) maximum displacement of 1 × 10⁻³ Å, d) maximum force of 0.03 eV/Å, and e) maximum stress of 0.05 GPa. The computation results are presented in Fig. S8.

Supporting Figures

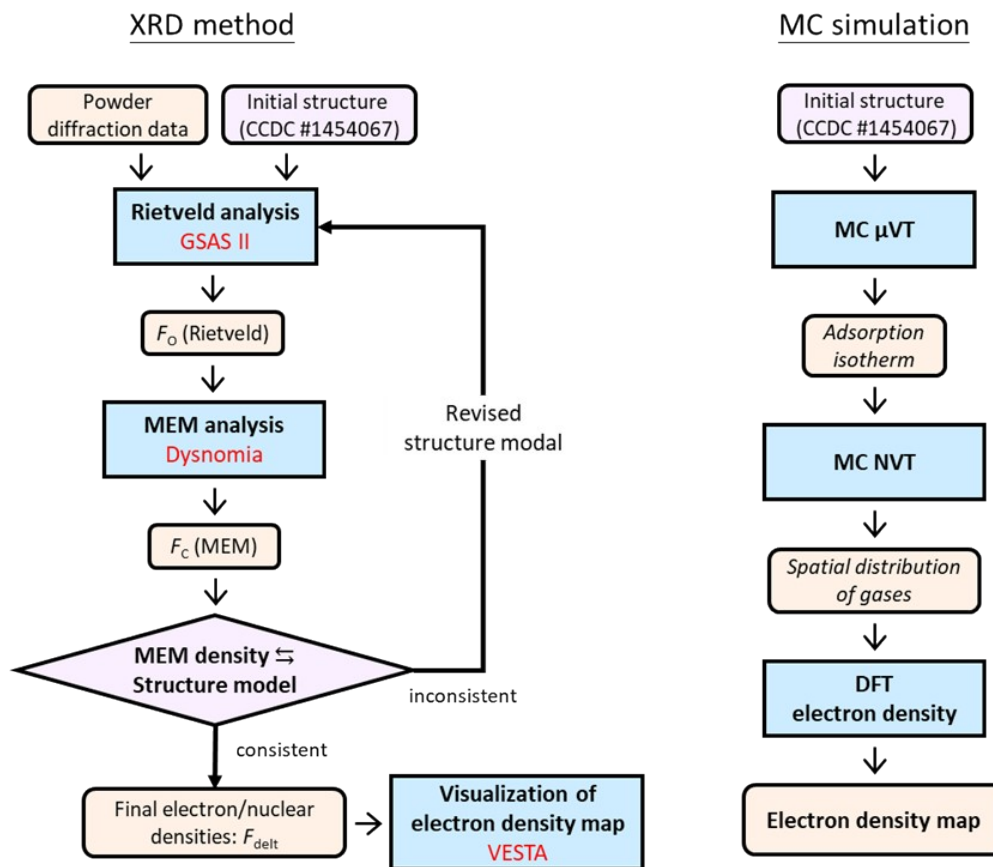


Fig. S1 Flow chart of proposed XRD-based method (left panel) and MC simulation (right panel). The observed structure factor (F_o), calculated structure factor (F_c), and difference Fourier map (F_{delt}) were calculated using the MEM/Rietveld analysis. F_{delt} was computed by subtracting F_c from F_o . For the XRD-based method, an electron density map of the gas species in the MOF structure was calculated based on F_{delt} .

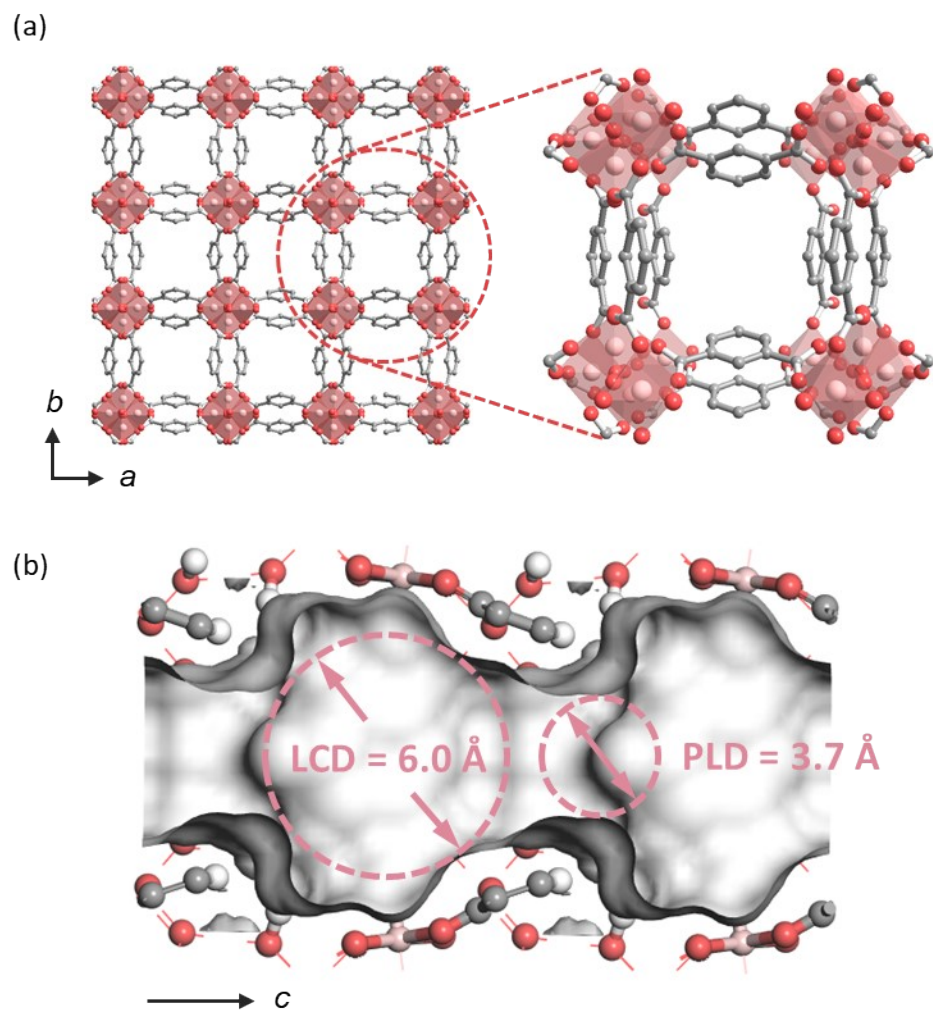


Fig. S2 Perspective view of CAU-10-H along (a) a - b plane and (b) b - c plane. The LCD and PLD are illustrated in b.

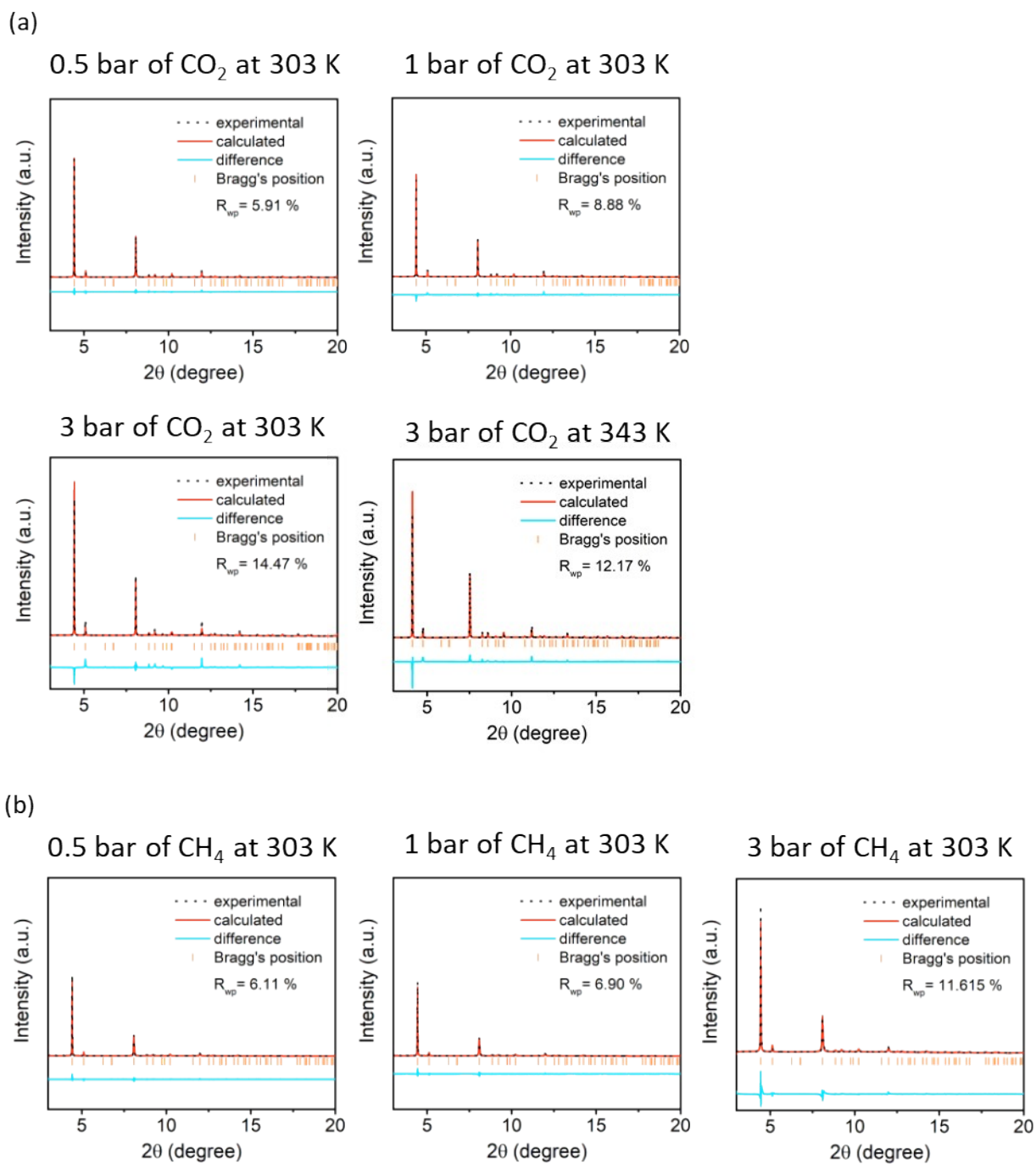


Fig. S3 Results of the Rietveld refinement for the powder XRD patterns of CAU-10-H measured under atmospheres of (a) CO₂ and (b) CH₄.

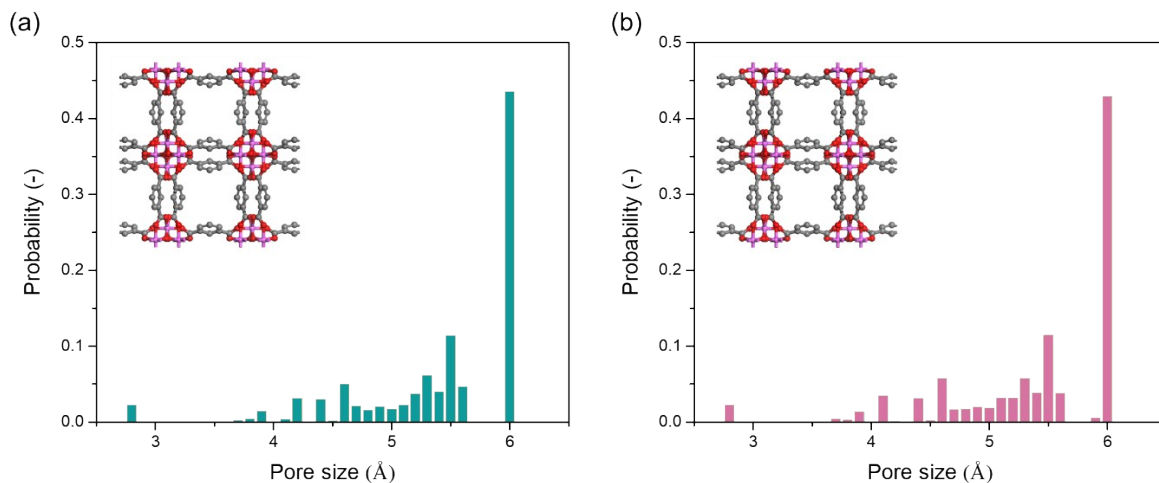


Fig. S4 Pore size distributions of CAU-10-H under vacuum and that under 3 bar of CO₂ at 303 K. These distributions were calculated based upon the CIFs obtained from the Rietveld refinement. The pore size calculations were conducted using an open-source package, Zeo++, with hypothetical spheres (2.2 Å in diameter) as a probe.

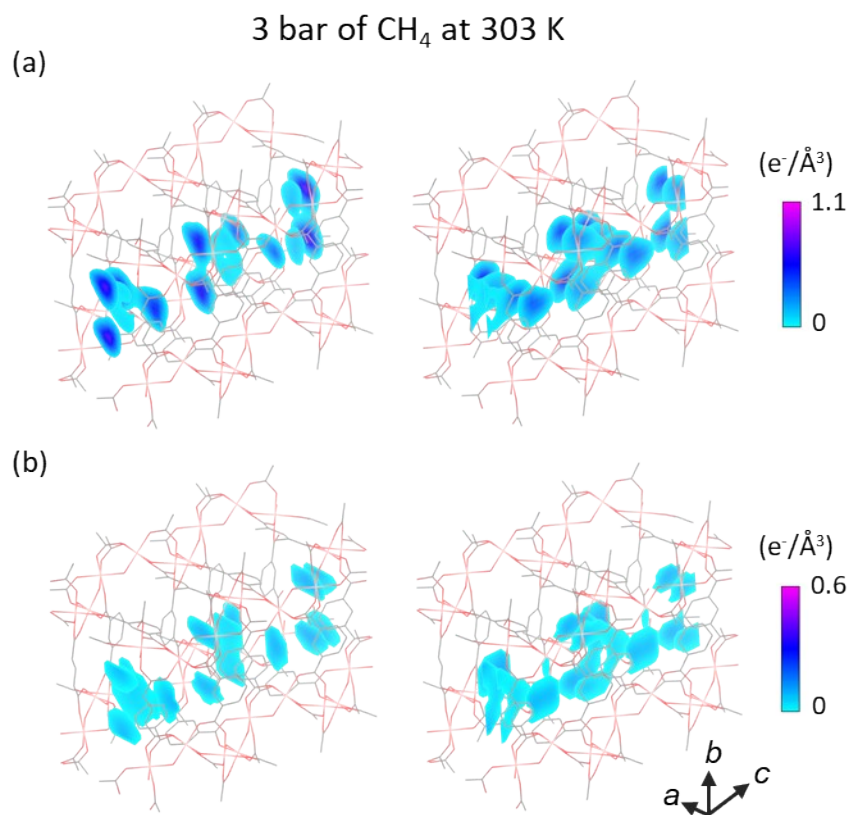


Fig. S5 Electron density maps of CH₄ adsorbed on CAU-10-H under 3 bar at 303 K derived using (a) MC- and (b) XRD-based methods for slices on *a-b* plane (left) and *b-c* plane (right).

3 bar of CH₄ at 303 K

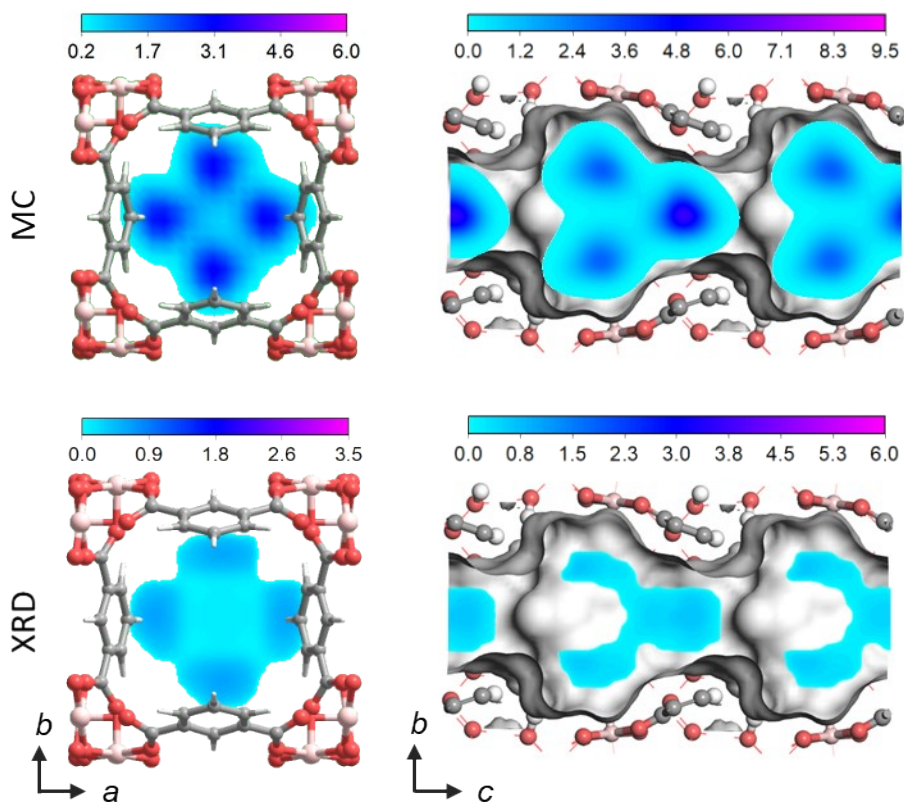


Fig. S6 Integral of the electron density of CH₄ along crystallographic *c*- and *a*-axis adsorbed on CAU-10-H under 3 bar at 303 K derived using the MC- and XRD-based methods. The color bars represent electron density in units of e⁻/Å².

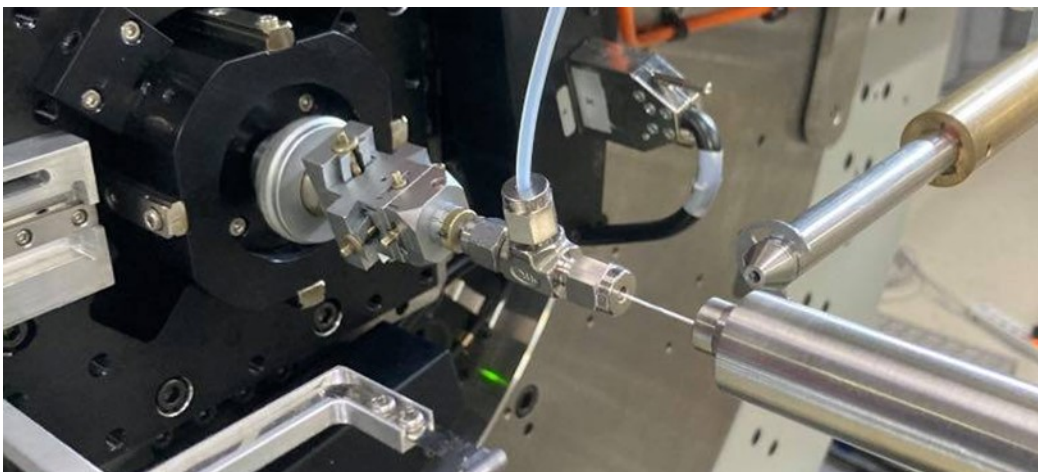


Fig. S7 Photographic image of the setup for the XRD experiments discussed in this study.

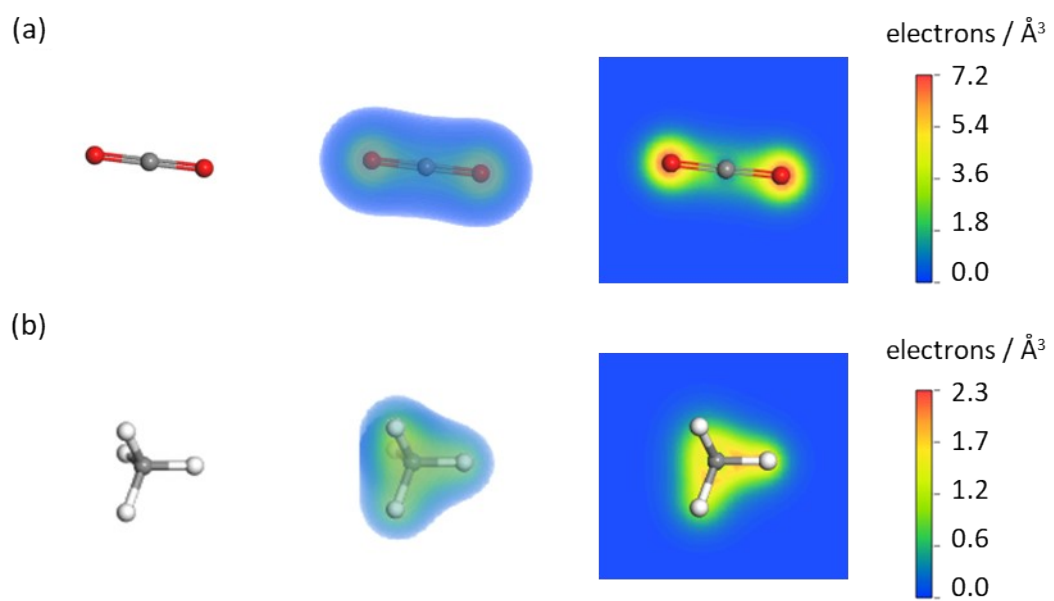


Fig. S8 Electron density maps of (a) CO_2 and (b) CH_4 obtained using DFT calculations in the CASTEP module of the Materials Studio software package.

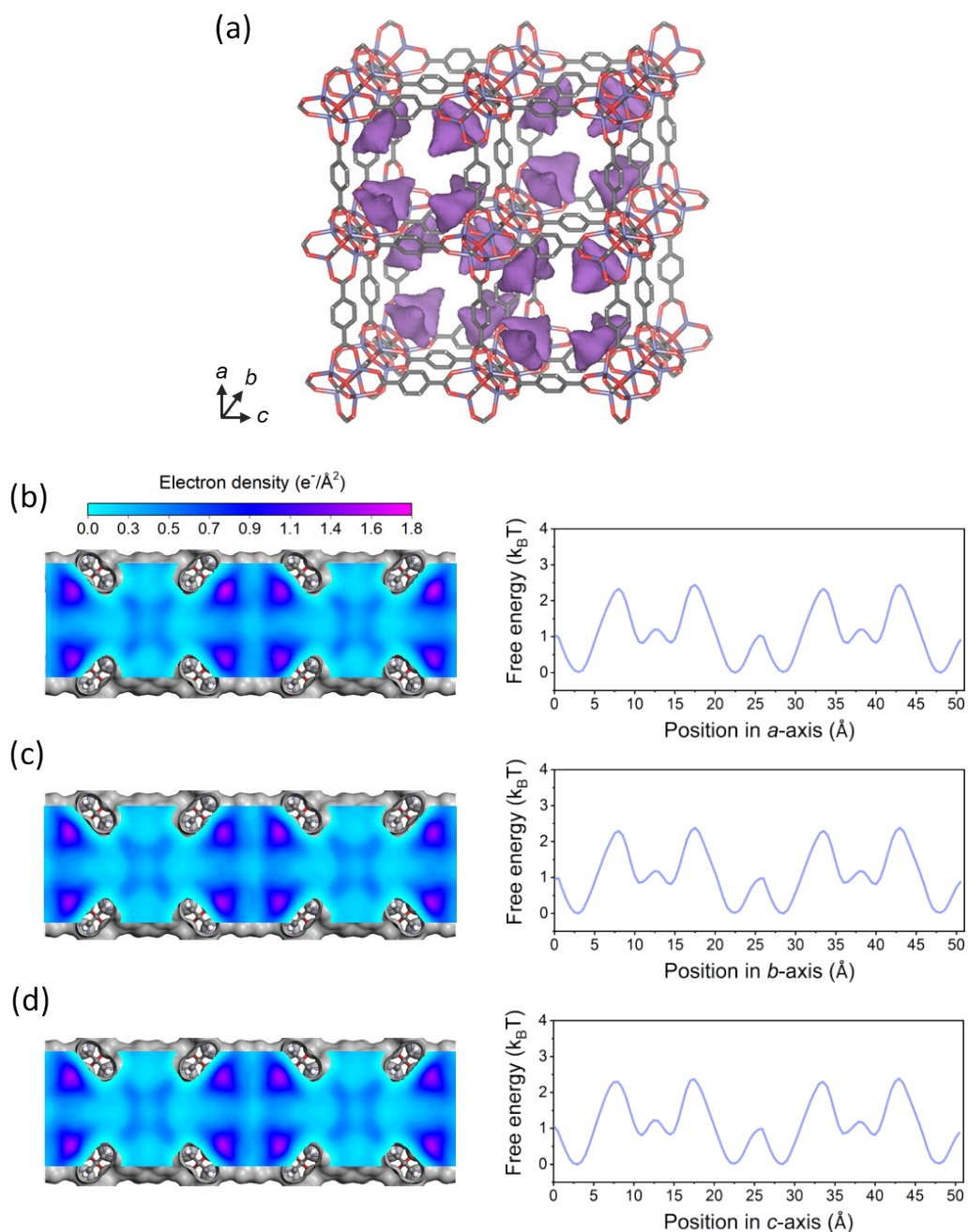


Fig. S9 (a) Illustration of crystal structure of MOF-5 with 3D interconnected channels. The Integral of electron density of CH₄ and the derived free energy profiles along crystallographic (b) *a*- (c) *b*- and (d) *c*-axis of MOF-5 derived using the MC-based method. The temperature was set to be 303 K. The free energy profiles along the three axes looked highly similar because of the cubic crystal of MOF-5.

Supporting tables

Table S1 Previous reports on the use of single-crystal or powder X-ray diffraction for the investigation of gas adsorption in MOFs.

Reference number in the main text	Adsorbent	Adsorbate	Single-crystal or powder diffraction	Investigation on free energy profile	Investigation on free energy profile self-diffusivity
[22]	IRMOF-74-V-hex	Ar	Single-crystal	No	No
[23]	PCN-224, ZIF-412, IRMOF-74-V-hex	Ar, N ₂ , O ₂	Single-crystal	No	No
[24]	[Zn ₄₁ O(bdc) ₃] _n , [Zn ₂ (bdc) ₂ -dabco] _n	Toluene, DMF	Single-crystal	No	No
[25]	MOF-1004, UiO-66	DMF	Single-crystal	No	No
[30]	Cu ₂ (pzdc) ₂ (pyz) ₂ ·2H ₂ O	C ₂ H ₂	Powder	No	No
[32]	CPL-1	O ₂	Powder	No	No
[26]	FMOF-1	N ₂	Single-crystal	No	No
[27]	Sc ₂ (O ₂ CC ₆ H ₄ CO ₂) ₃	CO ₂ , CH ₄ , C ₂ H ₆	Single-crystal	No	No
[28]	MOF-5	Ar, N ₂	Single-crystal	No	No
[29]	NbOFFIVE-1-Ni	Propane, propylene	Single-crystal	No	No
[31]	PCN-200	CO ₂	Powder	No	No

Table S2 Lattice parameters of CAU-10-H under CO₂ or CH₄ obtained from the Rietveld refinement. The indices for the fitting quality, expressed by goodness-of-fit (GOF) and weighted profile R-factor (R_{wp}), are also presented.

Pressure	Unit cell parameter			GOF	R _{wp}
	$a = b$ (Å)	c (Å)	$\alpha = \beta = \gamma$ (°)		
CO ₂ _0.5bar_303K	21.49	10.33	90	4.14	5.91
CO ₂ _1bar_303K	21.48	10.35	90	6.16	8.88
CO ₂ _3bar_303K	21.47	10.37	90	9.82	14.47
CO ₂ _3bar_343K	21.51	10.36	90	8.93	12.17
CH ₄ _0.5bar_303K	21.46	10.31	90	4.01	6.11
CH ₄ _1bar_303K	21.45	10.31	90	4.52	6.90
CH ₄ _3bar_303K	21.46	10.30	90	7.59	11.62

Table S3 Lennard-Jones parameters used in MC simulations.

Atom species	ε/k_B (K)	σ (Å)
O	48.1581	3.03315
C	47.8562	3.47299
H	7.64893	2.84642
Al	155.998	3.91105
CH4_sp3	158.5	3.72
O_co2	79.0	3.05
C_co2	27.0	2.80

Table S4 Self-diffusivity of methane in MOF-5 derived from the MC-based method. Results reported in the previous works are shown for comparison.

Method	Temperature (K)	Loading (mg g ⁻¹)	Self-diffusivity (m ² s ⁻¹)
MC	303	18	<i>a</i> -axis: 1.75×10^{-7}
			<i>b</i> -axis: 1.86×10^{-7}
			<i>c</i> -axis: 1.87×10^{-7}
PGF NMR ¹¹	298	120	1.7×10^{-7}
MD ¹²	300	3.25	3.1×10^{-8}

Note: the diffusivities of small gas molecules in MOF-5 were found to be insensitive to the loadings.^{13, 14}

Supplementary References

1. B. H. Toby and R. B. Von Dreele, *Journal of Applied Crystallography*, 2013, **46**, 544-549.
2. D. Fröhlich, E. Pantatosaki, P. D. Kolokathis, K. Markey, H. Reinsch, M. Baumgartner, M. A. van der Veen, D. E. De Vos, N. Stock, G. K. Papadopoulos, S. K. Henninger and C. Janiak, *Journal of Materials Chemistry A*, 2016, **4**, 11859-11869.
3. K. Momma, T. Ikeda, A. A. Belik and F. Izumi, *Powder Diffraction*, 2013, **28**, 184-193.
4. K. Momma and F. Izumi, *Journal of Applied Crystallography*, 2011, **44**, 1272-1276.
5. S. L. Mayo, B. D. Olafson and W. A. Goddard, *The Journal of Physical Chemistry*, 1990, **94**, 8897-8909.
6. M. D. Segall, P. J. D. Lindan, M. J. Probert, C. J. Pickard, P. J. Hasnip, S. J. Clark and M. C. Payne, *Journal of Physics Condensed Matter*, 2002, **14**, 2717-2744.
7. S. J. Clark, M. D. Segall, C. J. Pickard, P. J. Hasnip, M. I. J. Probert, K. Refson and M. C. Payne, *Zeitschrift für Kristallographie - Crystalline Materials*, 2005, **220**, 567-570.
8. J. P. Perdew, K. Burke and M. Ernzerhof, *Physical Review Letters*, 1996, **77**, 3865-3868.
9. D. Vanderbilt, *Physical Review B*, 1990, **41**, 7892-7895.
10. B. G. Pfrommer, M. Côté, S. G. Louie and M. L. Cohen, *Journal of Computational Physics*, 1997, **131**, 233-240.
11. F. Stallmach, S. Gröger, V. Künzel, J. Kärger, O. M. Yaghi, M. Hesse and U. Müller, *Angewandte Chemie International Edition*, 2006, **45**, 2123-2126.
12. L. Sarkisov, T. Düren and R. Q. Snurr, *Molecular Physics*, 2004, **102**, 211-221.
13. S. Amirjalayer and R. Schmid, *Microporous and Mesoporous Materials*, 2009, **125**, 90-96.
14. A. I. Skoulidas and D. S. Sholl, *The Journal of Physical Chemistry B*, 2005, **109**, 15760-15768.